Physical and Electrochemical Characterization of Nanocomposite Membranes of Nafion and Functionalized Silicon Oxide

Bradley P. Ladewig,[†,‡] Robert B. Knott,[§] Anita J. Hill,[⊥] James D. Riches,[#] John W. White,[||] Darren J. Martin,[†] João C. Diniz da Costa,[†] and Gao Qing Lu*[,†]

ARC Centre for Functional Nanomaterials, School of Engineering & AIBN, and Centre for Microscopy and Microanalysis, The University of Queensland, St Lucia QLD 4072, Australian Nuclear Science and Technology Organisation, Private Mail Bag 1, Menai, NSW 2234, CSIRO Manufacturing Science and Technology, Private Mail Bag 33, Clayton South, MDC, VIC 3169, and Research School of Chemistry, Australian National University, Canberra ACT 0200, Australia

Received December 4, 2006. Revised Manuscript Received January 12, 2007

Nafion nanocomposite membranes were prepared from Nafion 117 and a systematic range of organically functionalized silicon alkoxide precursors using an *in situ* sol gel synthesis technique. The physical structure of the resulting nanocomposite membranes were characterized using small and wide-angle X-ray scattering, small angle neutron scattering, positron annihilation lifetime spectroscopy, and transmission electron microscopy. A structural model is proposed for three typical nanocomposite membranes (Nafion-TEOS, Nafion-MPTMS and Nafion-MPMDMS). The proton and methanol transport properties of the membranes included in the model were evaluated by impedance spectroscopy and pervaporation experiments, respectively, and correlated to their composite microstructure. In particular, this model explains the increased selectivity for transport over protons for nanocomposite membranes produced using (3-mercaptopropyl)methyldimethoxysilane as the silicon alkoxide precursor, which is more than six times higher than that of Nafion 117.

Introduction

Direct methanol fuel cells (DMFC) are seen as an attractive potential replacement for lithium-ion batteries in portable devices because of their potentially high-energy density, which may be up to 10 times that of conventional secondary batteries.[1] For this reason, they are being considered for applications in laptop computers, mobile phones, and military devices.[2] A major drawback is the high methanol permeability of Nafion, which is the most commonly used membrane in DMFCs.[3] This crossover of methanol from the anode to the cathode of the DMFC leads to reduced cell potential and efficiency[4] and is a major impediment to widespread DMFC commercialization.

It is well-known that incorporating filler particles into polymer membranes can dramatically alter their transport properties,[5] and one approach to decreasing the methanol permeability of Nafion membranes is to incorporate silicon oxide nanoparticles, which hinder the transport of methanol through the composite material. The production of Nafion-silicon oxide composite membranes can be achieved by a number of different techniques. The first one is mixing silicon oxide particles with the polymer in solution and casting the composite membrane.[6−11] Second, one can use silicon alkoxide precursors and sol−gel chemistry to produce silicon oxide particles in Nafion solution and casting these to form composite membranes.[12−18] The third technique is to form silicon oxide particles in the membrane by in situ sol−gel synthesis.[19−27] This technique was chosen in this work to

* Corresponding author. E-mail: maxlu@uq.edu.au.
† ARC Centre for Functional Nanomaterials, The University of Queensland.
‡ Current address: Laboratoire des Sciences du Génie Chimique, CNRS-ENSIC, 1 rue Grandville, BP 20451, 54001 Nancy Cedex, France.
§ Australian Nuclear Science and Technology Organisation (ANSTO).
⊥ CSIRO Manufacturing Science and Technology.
Centre for Microscopy and Microanalysis, The University of Queensland.
|| Research School of Chemistry, Australian National University.

(1) Service, R. F. *Science* **2002**, *296*, 1222.
(2) Cowey, K.; Green, K. J.; Mepsted, G. O.; Reeve, R. *Curr. Opin. Solid State Mater. Sci.* **2004**, *8*, 367.
(3) Mauritz, K. A.; Moore, R. B. *Chem. Rev.* **2004**, *104*, 4535.
(4) Deluca, N. W.; Elabd, Y. A. *J. Polym. Sci. Polym. Phys.* **2006**, *44*, 2201.
(5) Giannelis, E. P. *Adv. Mater.* **1996**, *8*, 29.
(6) Staiti, P.; Arico, A. S.; Baglio, V.; Lufrano, F.; Passalacqua, E.; Antonucci, V. *Solid State Ionics* **2001**, *145*, 101.
(7) Antonucci, P. L.; Arico, A. S.; Creti, P.; Ramunni, E.; Antonucci, V. *Solid State Ionics* **1999**, *125*, 431.
(8) Antonucci, V.; Arico, A. S. European Patent EP 0 926 754 A1, 1999.
(9) Dimitrova, P.; Friedrich, K. A.; Stimming, U.; Vogt, B. *Solid State Ionics* **2002**, *150*, 115.
(10) Dimitrova, P.; Friedrich, K. A.; Vogt, B.; Stimming, U. *J. Electroanal. Chem.* **2002**, *532*, 75.
(11) Stonehart, P.; Watanabe, M. US Patent 5,523,181. 5,523,181, 1996.
(12) Li, C. N.; Sun, G. Q.; Ren, S. Z.; Liu, J.; Wang, Q.; Wu, Z. M.; Sun, H.; Jin, W. *J. Membr. Sci.* **2006**, *272*, 50.
(13) Arico, A. S.; Baglio, V.; Antonucci, V.; Nicotera, I.; Oliviero, C.; Coppola, L.; Antonucci, P. L. *J. Membr. Sci.* **2006**, *270*, 221.
(14) Jiang, R. C.; Kunz, H. R.; Fenton, J. M. *J. Membr. Sci.* **2006**, *272*, 116.
(15) Kim, H.-J.; Shul, Y.-G.; Han, H. *J. Power Sources* **2006**, *158*, 137.
(16) Kim, Y. J.; Choi, W. C.; Woo, S. I.; Hong, W. H. *J. Membr. Sci.* **2004**, *238*, 213.
(17) Miyake, N.; Wainright, J. S.; Savinell, R. F. *J. Electrochem. Soc.* **2001**, *148*, A905.
(18) Ren, S.; Sun, G.; Li, C.; Liang, Z.; Wu, Z.; Jin, W.; Qin, X.; Yang, X. *J. Membr. Sci.* **2006**, *282*, 450.
(19) Baradie, B.; Dodelet, J. P.; Guay, D. *J. Electroanal. Chem.* **2000**, *489*, 101.
(20) Deng, Q.; Moore, R. B.; Mauritz, K. A. *J. Appl. Polym. Sci.* **1998**, *68*, 747.
(21) Klein, L. C.; Daiko, Y.; Aparicio, M.; Damay, F. *Polymer* **2005**, *46*, 4504.

10.1021/cm0628698 CCC: $37.00
Published on Web 04/07/2007

Table 1. Silicon Content of Nafion, Test SiO_2, and Nafion Composite Membranes as Determined by Inductively Coupled Plasma Atomic Emission Spectrophotometry

sample	weight (mg)	digest Si (μg mL^{-1})	Si in sample (wt %)	Si/inorganic
Nafion	115.3	0.1	0.00	
test SiO2	12.0	112.4	46.83	
Nafion-TEOS 6.0 wt %	113.2	25.2	1.11	0.19
Nafion-TEOS 10.0 wt %	96.9	73.7	3.80	0.38
Nafion-MPTMS 11.6 wt %	90.2	50.5	2.80	0.24
Nafion-MPTMS 14.4 wt %	59.9	64.8	5.41	0.38
Nafion-MPMDMS 7.4 wt %	120.4	29.8	1.24	0.17
Nafion-MPMDMS 11.3 wt %	106.5	38.4	1.80	0.16

produce a range of nanocomposite membranes using systematically varied silicon alkoxide precursors. The resulting membranes are characterized extensively to gain a detailed understanding of the resulting composite microstructure and their transport properties.[28]

A mechanistic model is proposed to describe the structure of three of the Nafion composite systems and relate the structural differences to the measured proton conductivity and methanol permeability of these materials, providing an understanding of the synthesis−structure−property relationship for this class of materials.

Experimental Section

Materials. Nafion 117 was obtained from CG Processing, Inc., and cleaned by placing it in a 3% H_2O_2 solution at 60 °C for 60 min, rinsing it with distilled water, placing it in 1 M H_2SO_4 at 60 °C for 60 min, rinsing it with distilled water, and then placing it in distilled water at 60 °C for 60 min. Cleaned membranes were dried at 100 °C overnight and weighed to determine their initial dry weight before inorganic modification. Tetraethyl orthosilicate (TEOS), (3-mercaptopropyl)trimethoxysilane (MPTMS), (3-mercaptopropyl)methyldimethoxysilane (MPMDMS), dimethyldimethoxysilane (DMDMS), and methyltriethoxysilane (MTES) were obtained from Aldrich and used as received.

Nanocomposite Membrane Synthesis. The technique used in this work is based on the method first proposed by Mauritz et al.,[26] who described the use of the phase-separated morphology of Nafion as a structure-directing template for the reaction of TEOS with water, catalyzed by the immobilized sulfonic acid groups in the hydrophilic clusters. This technique has been modified with the aim of producing smaller inorganic particles by limiting the quantity of water available for the reaction and confining it to the cluster regions. The membranes were exposed to a constant relative humidity of 27% over a saturated salt solution of KCl[29] for 60 min, then placed into a 1:8 (mol/mol) solution of silicon alkoxide/ethanol for 60 s. After removal from the silicon alkoxide solution, the membranes were rinsed thoroughly with ethanol to remove any reactants on the membrane surface and dried in an oven at 100 °C for 60 min. They were then removed and weighed to determine the weight percent inorganic uptake. This process of exposure to a humid atmosphere, immersion in silicon alkoxide solution, and drying was repeated until the desired inorganic content was achieved.

Membranes produced from MPTMS and MPMDMS were further treated with 30% H_2O_2 at 60 °C for 60 min to oxidize surface thiol groups to sulfonic acid groups,[30] after which they were again rinsed with distilled water, dried at 100 °C for 60 min, and weighed to determine the final inorganic content.

Membrane Characterization. The silicon content of the membranes was determined as follows: 50−100 mg of membrane materials was mixed with 500 mg of Na_2O_2 and fused in a platinum crucible at 500 °C for 30 min to oxidize the sample. The fusion contents were dissolved in boiling deionized water for 30 min, diluted to 50 mL, and filtered. The silicon content of the solution was analyzed using an inductively coupled plasma atomic emission spectrophotometer (ICP-AES). The fusion process was tested for recovery using a reference SiO_2 sample.

Proton conductivity was measured using a two electrode transverse impedance technique. The blocking electrodes were made of gold-plated copper, 8 mm in diameter, and pressed together with a force of 22.2 N. Samples were soaked overnight in distilled water before being fully submerged in distilled water at 50 °C for testing. A Solartron 1260 frequency response analyzer applied a sinusoidal voltage of 10 mV amplitude over the frequency range $1-10^7$ Hz, and the proton conductivity, σ, was calculated according to eq 1[31]

$$\sigma = \frac{l}{(R - R_0)A} \tag{1}$$

where l is the membrane thickness, A the electrode contact area, R the measured membrane resistance (taken as the membrane impedance at zero-phase angle), and R_0 the cell closed circuit resistance. The proton conductivity of each membrane was measured three times, in different areas of the membrane, and the results were averaged.

Methanol permeability was determined using a pervaporation technique, in which a 1:1 (mol/mol) CH_3OH/H_2O solution was circulated over one side of the membrane using a peristaltic pump and 60 mL of He min^{-1} was passed over the other side, evaporating any permeate, which was subsequently condensed out in a liquid nitrogen cooled condenser. The pervaporation cell was maintained at 50 °C. Three consecutive samples of condensate, collected over 30 min each, were weighed to determine the bulk flux through the membrane. The composition of the condensate was determined using a gas chromatograph (Shimadzu GC 17A) equipped with a capillary column (HP-Plot U) and a thermal conductivity detector.

Small angle neutron scattering (SANS) experiments were conducted on the Australian nuclear science and technology

(22) Mauritz, K. A. *Macromolecules* **1989**, *22*, 4483.
(23) Mauritz, K. A.; Payne, J. T. *J. Membr. Sci.* **2000**, *168*, 39.
(24) Mauritz, K. A.; Stefanithis, I. D. *Macromolecules* **1990**, *23*, 1380.
(25) Mauritz, K. A.; Stefanithis, I. D.; Davis, S. V.; Scheetz, R. W.; Pope, R. K.; Wilkes, G. L.; Huang, H. H. *J. Appl. Polym. Sci.* **1995**, *55*, 181.
(26) Mauritz, K. A.; Storey, R. F.; Jones, C. K. In *Multiphase Polymers: Blends and Ionomers*; Utracki, L. A., Weiss, R. A., Eds.; ACS Symposium Series No. 395; American Chemical Society: Washington, DC, 1989; pp 401−417.
(27) Xu, W. L.; Lu, T. H.; Liu, C. P.; Xing, W. *Electrochim. Acta* **2005**, *50*, 3280.
(28) Ladewig, B. P.; Knott, R. B.; Martin, D. J.; Diniz, da Costa, J. C.; Lu, G. Q. *Electrochem. Commun.* **2007**, *9*, 781.
(29) Acheson, D. T. In *Humidity and Moisture: Measurement and Control in Science and Industry*; Wexler, A., Ed.; Reinhold: New York, 1965; Vol. 4.
(30) Cano-Serrano, E.; Blanco-Brieva, G.; Campos-Martin, J. M.; Fierro, J. L. G. *Langmuir* **2003**, *19*, 7621.
(31) Khiterer, M.; Loy, D. A.; Cornelius, C. J.; Fujimoto, C. H.; Small, J. H.; McIntire, T. M.; Shea, K. J. *Chem. Mater.* **2006**, *18*, 3665.

Table 2. Molecular Weights for Unhydrolyzed, Hydrolyzed, and Completely Condensed Inorganic Precursors and the Corresponding Silicon Weight Fraction[a]

precursor	molecular/repeat unit formula	mol wt	Si wt fraction
TEOS	$Si(OCH_2CH_3)_4$	208.32	0.13
	$Si(OH)_4$	96.11	0.29
	SiO_2	60.08	0.47
MPTMS	$Si(OCH_3)(CH_2)_3SO_3H$	244.34	0.11
	$Si(OH)_3(CH_2)_3SO_3H$	202.26	0.14
	$Si(O)_{3/2}(CH_2)_3SO_3H$	175.24	0.16
	$Si(O)_{3/2}(CH_2)_3SH$	127.24	0.22
MPMDMS	$Si(OCH_3)_2CH_3(CH_2)_3SO_3H$	228.34	0.12
	$Si(OH)_2CH_3(CH_2)_3SO_3H$	200.29	0.14
	$SiOCH_3(CH_2)_3SO_3H$	182.27	0.15
	$SiOCH_3(CH_2)_3SH$	134.27	0.21

[a] For the two thiol-functionalized precursors, the molecular weights for the unhydrolyzed, hydrolyzed, and completely condensed states assume complete oxidation of the −SH groups to $-SO_3H$ after treatment with H_2O_2. Also included is the molecular weight of the completely condensed, unoxidized state.

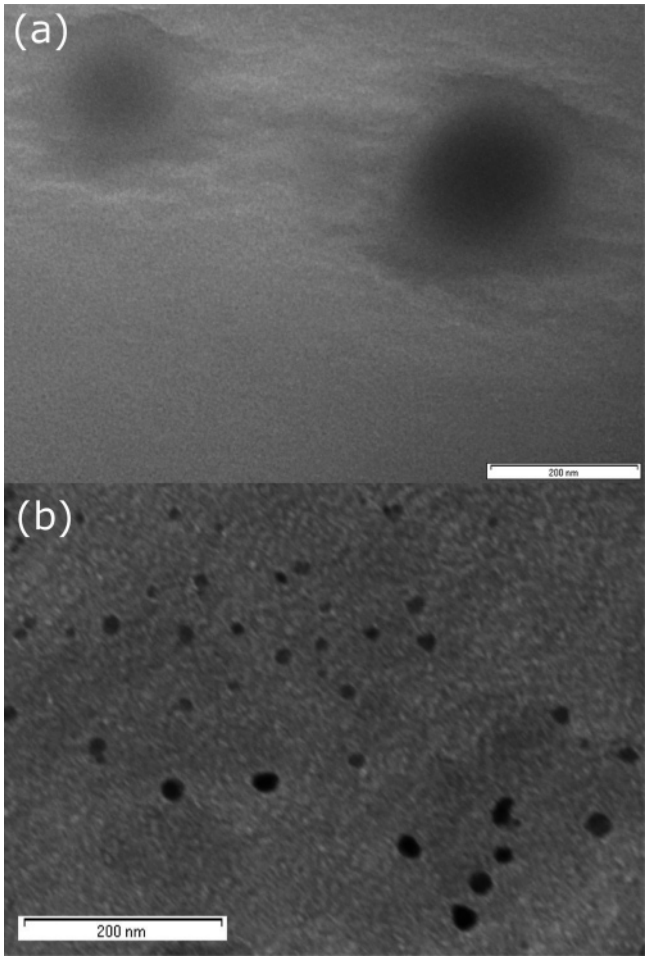

Figure 1. TEM images of (a) 1.3 wt % Nafion-TEOS and (b) 11.1 wt % Nafion-TEOS nanocomposite membranes.

organization (ANSTO) SANS instrument with a sample aperture of 10 mm diameter, neutron wavelength of 3.5 Å, and sample-to-detector distance of 4800 mm (total q range 0.01 $Å^{-1} < q < 0.15$ $Å^{-1}$). Here, q is the scattering vector defined by $q = 4\pi \sin\theta/\lambda$, where 2θ is the scattering angle. The total data collection time for each sample was 4 h. The raw data were corrected for backgrounds according to eq 2

$$I_{COR} = (I_{SAM} - I_{BGD}) - \frac{T_{SAM}}{T_{EMP}}(I_{EMP} - I_{BGD}) \qquad (2)$$

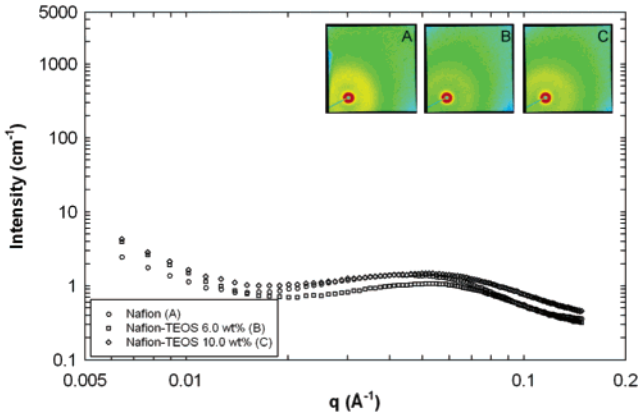

Figure 2. SAXS profile for Nafion-TEOS nanocomposite membranes.

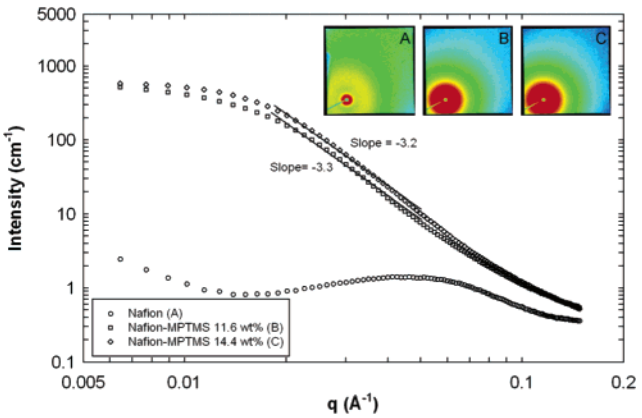

Figure 3. SAXS profile for Nafion-MPTMS nanocomposite membranes.

where I is the scattered intensity, T is the transmission, COR is corrected, SAM is raw sample, BGD is raw background (blocked beam), and EMP is empty cell. For these experiments, the empty cell was three thicknesses of aluminum foil. The corrected two-dimensional patterns were then radially integrated around $q = 0$ to produce one-dimensional SANS profiles. The intensity data were placed on an absolute scale (±5%) by comparing them with the scattered intensity from a secondary standard (porous silica $R_g = 29.9 \pm 0.5$ Å, $I(0) = 2358 \pm 20$, $d\Sigma/d\Omega = 27$ cm^{-1}).

Small-angle X-ray scattering (SAXS) was conducted on the ChemMatCARS SAXS/WAXS instrument at the Argonne Advanced Photon Source, Chicago. The sample was mounted on a computer-controlled sample changer on the SAXS/WAXS instrument and exposed to the X-ray beam for 1 s.[32] The background intensity was collected for a sample-free configuration for the same exposure time. The X-ray wavelength was 1.5 Å and the beam energy was 8.2656 keV. The sample-to-detector distance was 1864 mm and the beam dimensions at the sample position were 500 × 500 μm^2. The detector was a CCD, with an active area of 940 × 940 mm^2 and pixel size of 92 × 92 μm^2.

Positron annihilation lifetime spectroscopy (PALS) experiments were performed using an automated EG&G Ortec fast−fast coincidence system with a resolution of 240 ps. Four thicknesses of the Nafion composite sample were placed on either side of a $^{22}NaCl$ source (2 mm diameter 25 μCi spot sandwiched between two 2.54 μm titanium foils). Data were collected and analyzed using the PFPOSFIT program. At least five spectra of 30 000 peak counts were collected, with each spectrum taking approximately 1 h to collect. The PALS parameters for the membranes did not change

(32) Cookson, D.; Kirby, N.; Knott, R.; Lee, M.; Schultz, D. *J. Synchrotron Radiat.* **2006**, *13*, 440.

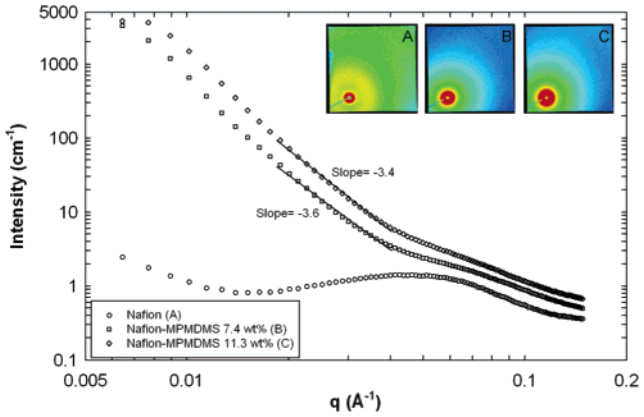

Figure 4. SAXS profile for Nafion-MPMDMS nanocomposite membranes.

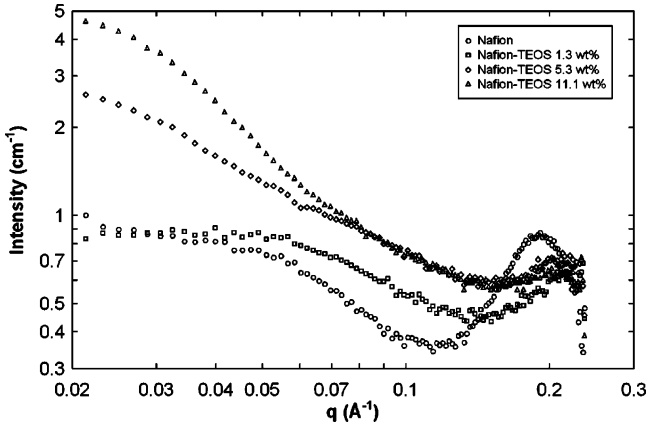

Figure 5. SANS profile for Nafion-TEOS nanocomposite membranes.

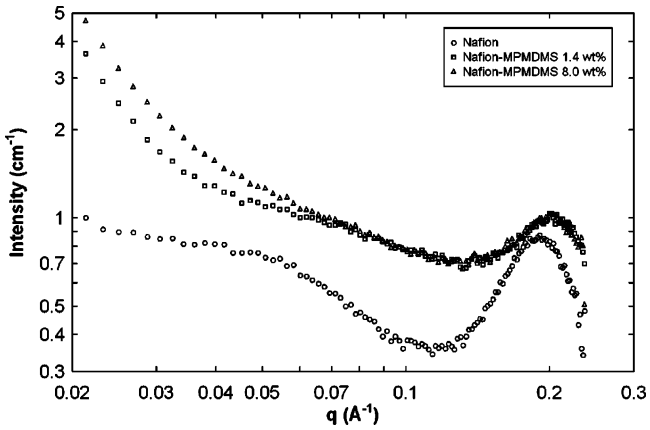

Figure 6. SANS profile for Nafion-MPMDMS nanocomposite membranes.

as a function of contact time with the source. No source correction was used. Three lifetimes were fitted with the shortest fixed to 125 ps, characteristic of p-Ps self-annihilation. Assuming spherical free volumes, eq 3 gives the analytical relationship between the o-Ps lifetime τ_3 and the free volume radius R

$$\tau_3^{-1} = 2\left[1 - \frac{R}{R_0} + \frac{1}{2\pi}\sin\left(\frac{2\pi R}{R_0}\right)\right] (\text{ns}^{-1}) \qquad (3)$$

where $R_0 = R + \Delta R$. ΔR is an empirical parameter, the best known value of which is 1.66 Å.[33]

Transmission electron microscopy (TEM) samples of size 1 mm × 3 mm were cooled in the chuck of a Leica UC6 cryoultramicrotome. Cross-sections of 80 nm thickness were cut at −120 °C using a glass knife and then transferred to 400 mesh copper grids and allowed to warm to room temperature. Samples were then analyzed using a JEOL TEM at an accelerating voltage of 80 kV and a FEI Tecnai F20 field emission gun TEM/STEM, operated at 200 kV.

Results and Discussion

The results of ICP-AES analysis of the Nafion composite membranes are presented in Table 1. Digest Si is the silicon concentration in the diluted digest liquor as reported by the ICP-AES, and the Si/inorganic value reported in the final column is the ratio of the weight percent silicon measured by ICP-AES to the weight percent inorganic measured gravimetrically after the membrane synthesis.

The technique used to measure the silicon content appears to provide accurate compositional data. The Nafion sample exhibited negligible silicon content, whereas a test of a quantity of pure SiO_2 on the same order of magnitude as was present in the composite membranes returned 46.83 wt % Si, which is equivalent to 98.5% recovery. The values for the Si/inorganic ratio should be considered in the context of Table 2, which details the molecular weights for the unhydrolyzed, hydrolyzed, and completely condensed states of the inorganic precursors and the corresponding silicon weight fraction. For all the precursors, the lowest possible value of Si/inorganic is that of the unhydrolysed precursor, at 0.13, 0.11, and 0.12 for TEOS, MPTMS, and MPMDMS, respectively. The highest is that of the fully condensed state, although for MPTMS and MPMDMS, the extent of oxidation of the thiol group to sulfonic acid must also be considered, as the difference in molecular weight between the unoxidized and oxidized states is significant. It should be noted that the oxidation conditions utilized in the synthesis are expected to produce near-complete oxidation of the thiol group.[30]

Considering first the Nafion composite membranes synthesized using TEOS as the inorganic precursor, the 6.0 wt % composite yielded a Si/inorganic ratio of 0.19. According to the values in Table 2, this corresponds to TEOS in a partially hydrolyzed, noncondensed state. This is consistent with the TEM micrograph of a Nafion-TEOS 1.3 wt % composite, Figure 1a, which shows regions of higher electron density that are not fully densified, surrounded by the host Nafion polymer. The regions of higher electron density are attributed to agglomeration of partially hydrolyzed TEOS molecules. The low extent of hydrolysis may be explained by the limited water present using this synthesis technique. The Nafion-TEOS 10.0 wt % composite gave a Si/inorganic ratio of 0.38, which is in the region of fully hydrolyzed TEOS that is partially condensed. Figure 1b, which is a TEM micrograph of a Nafion-TEOS 11.1 wt % composite, appears to confirm that the TEOS in this sample is much more condensed, as the silicon-rich regions show a much higher contrast to the surrounding Nafion polymer. From these observations, it appears that as the synthesis of Nafion-TEOS composite membranes proceeds and the agglomerated regions of the inorganic precursor are sequentially exposed to water vapor and more precursor solution and then dried, the

(33) Mallon, P. E. In *Positron and Positronium Chemistry*; Jean, Y. C., Mallon, P. E., Schrader, D. M., Eds.; World Scientific: Singapore, 2003.

Table 3. Summary of Peak Positions from SANS Experiments on Nafion, Nafion-TEOS, and Nafion-MPMDMS Nanocomposite Membranes

membrane	inorganic content (wt %)	q_{max} (Å^{-1})	d (Å)
Nafion		0.19	33
Nafion-TEOS	1.3	0.23	27
Nafion-TEOS	5.3	0.21	30
Nafion-TEOS	11.1	0.23	27
Nafion-MPMDMS	1.4	0.20	31
Nafion-MPMDMS	8.0	0.20	31

Table 4. Summary of Results from the Deconvolution of Wide-Angle X-ray Scattering Data, Where q_{am} is the Position of the Amorphous Peak, q_{cr} is the Position of the Crystalline Peak, and W_{cr} is the Weight-Averaged Crystallinity

membrane	inorganic content (wt %)	q_{am} (Å^{-1})	q_{cr} (Å^{-1})	W_{cr}
Nafion		1.09	1.22	0.48
Nafion-TEOS	1.3	1.12	1.24	0.25
Nafion-TEOS	5.3	1.12	1.24	0.29
Nafion-TEOS	11.1	1.12	1.24	0.29
Nafion-MPMDMS	1.4	1.13	1.24	0.28
Nafion-MPMDMS	4.6	1.12	1.25	0.32
Nafion-MPMDMS	8.0	1.13	1.25	0.27

network becomes more condensed.

The Nafion-MPTMS composite membranes show an interesting result in their Si/inorganic ratio, as the values obtained (0.24 and 0.38 for the 11.6 and 14.4 wt % composites, respectively) are somewhat higher than is assumed possible. It is shown in Table 2 that fully condensed and oxidized MPTMS should have a Si/inorganic ratio of 0.16, or 0.22 if the thiol groups remained unoxidized. A possible explanation for this discrepancy would be if either the polymer or inorganic phase lost some mass during the synthesis procedure. An example of this may be if some of the propyl thiol side chains were oxidized from the central Si atom during the hydrogen peroxide treatment, leaving a silanol group. This would effectively increase the Si/inorganic ratio.

It is also seen that, similarly to the Nafion-TEOS composites, there is an increase in the Si/inorganic ratio with increasing overall inorganic loading, which again suggests that the degree of condensation is higher in the samples that have undergone more repetitions of the synthesis procedure.

Finally, the Nafion-MPMDMS composites display Si/inorganic values in very close agreement with those expected for the completely condensed precursor, with the majority of the thiol groups oxidized. Interestingly, the values are similar for both the low and high inorganic loadings and do not increase with loading as for the Nafion-TEOS and Nafion-MPTMS composites. This result is consistent with the ^{29}Si Solid-state NMR results of Young et al.,[34] in which it was shown that a bifunctional silicon alkoxide precursor (in that case, diethoxydimethylsilane) incorporated into Nafion membranes using a similar synthesis technique undergoes complete hydrolysis and condensation.

Figures 2−4 show the SAXS profiles of Nafion-TEOS, Nafion-MPTMS, and Nafion-MPMDMS nanocomposite membranes, respectively, over the range $q = 0.006-0.12$ Å^{-1}.

The raw 2D SAXS pattern for the membrane under investigation is presented inset in each figure; the pattern has been corrected for detector spatial distortion. The color (log) scale indicates the number of X-ray photons collected in each pixel of the 1024 × 1024 pixel detector and is autoscaled between the maximum and minimum counts per pixel. The 2D data were radially averaged, and the background subtracted using the SAXS15ID software[32] and the scattered intensity was placed on an absolute scale using glassy carbon as a secondary standard. The scattering profile of Nafion is included in each graph for comparison, and all graph ordinates have the same scale.

The ionomer peak is not visible in Figures 2−4, because as shown by Rubatat et al.,[35] the ionomer peak occurs at higher q. There is a broad peak visible in the plots, which for Nafion and the Nafion-TEOS composite membranes occurs at around $q = 0.05$ Å^{-1}. This is described by Rubatat et al.[35] as the "matrix knee", the physical meaning of which is not known.

Considering the general form of the scattering curves in Figure 2, it can be seen that the Nafion-TEOS composite membranes with 6.0 and 10.0 wt % loading produced essentially the same scattering curves as Nafion, although with a slight upturn in intensity in the region $q = 0.006-0.012$ Å^{-1}. This stands in strong contrast to the scattering curves for Nafion-MPTMS in Figure 3, where a strong upturn in the scattered intensity is seen over the range $q = 0.015-0.1$ Å^{-1}, which then plateaus off at $q = 0.006-0.015$ Å^{-1}. Similarly, the Nafion-MPMDMS composites show a strong upturn in the scattered intensity beginning at around $q = 0.016$ Å^{-1} and extending right down to $q = 0.006$ Å^{-1}.

Assuming that the Nafion phase has the same density as bulk Nafion, 1.83 g cm^{-3},[36] that the inorganic components have a density of approximately 2.0 g cm^{-3}, [37] and that the chemical composition of the inorganic phases is the same as that derived from ICP-AES measurements, the X-ray scattering length density (SLD) differences for Nafion-TEOS, Nafion-MPTMS, and Nafion-MPMDMS systems were calculated to be 2.5, 2.7, and 2.8 × 10^{-6} Å^{-2}. The calculated values for the SLD differences are all quite similar, which suggests that there are variations in the quantity of scattering objects of the relevant size range contributing to the differences in the scattering curves of Nafion-TEOS compared to Nafion-MPTMS and Nafion-MPMDMS.

The structure of the inorganic phase in this instance may be represented by the mass-fractal model. It can be shown that for $1/R \ll q \ll 1/a$, the intensity is related to q by eq 4[38]

$$I(q) \propto q^{-d} \tag{4}$$

where d is the fractal dimension, R is the overall dimension of the particle, and a is the size of the basic building block of the structure (in this case, the atoms comprising the inorganic particles). For this study, those criteria are satisfied and this allows the slope of the scattering curves for the

(34) Young, S. K.; Jarrett, W. L.; Mauritz, K. A. *Polymer* **2002**, *43*, 2311.
(35) Rubatat, L.; Gebel, G.; Diat, O. *Macromolecules* **2004**, *37*, 7772.
(36) Oberbroeckling, K. J.; Dunwoody, D. C.; Minteer, S. D.; Leddy, J. *Anal. Chem.* **2002**, *74*, 4794.
(37) Madani, M. M.; MacQueen, R. C.; Granata, R. D. *J. Polym. Sci. Polym. Phys.* **1996**, *34*, 2767.
(38) Roe, R. J., *Methods of X-ray and Neutron Scattering in Polymer Science*; Oxford University Press: New York, 2000.

Table 5. Positron Annihilation Lifetime Spectroscopy Results for Nafion and Nafion Nanocomposite Membranes

membrane	inorganic content (wt %)	o-Ps lifetime, τ_3 (ns)	o-Ps intensity, I_3 (%)	nanovoid radius (Å)	nanovoid volume (Å^3)
Nafion 117[45]		2.79 ± 0.01	10 ± 0.3	3.49	178
Nafion 117		2.890 ± 0.03	9.360 ± 0.14	3.56	190
Nafion-MPTMS	6.8	2.823 ± 0.05	9.532 ± 0.17	3.52	182
Nafion-MPTMS	7.4	2.718 ± 0.01	9.127 ± 0.11	3.44	171
Nafion-MPMDMS	7.1	2.672 ± 0.04	8.654 ± 0.16	3.41	166
Nafion-MPMDMS	7.1	2.637 ± 0.08	8.825 ± 0.26	3.38	162
Nafion-DMDMS	3.4	2.914 ± 0.06	10.172 ± 0.25	3.58	192
Nafion-DMDMS	7.9	2.892 ± 0.03	11.239 ± 0.03	3.56	190
Nafion-MTES	9.6	2.920 ± 0.04	12.019 ± 0.32	3.58	192
Nafion-MTES	16.9	2.933 ± 0.02	12.781 ± 0.16	3.59	194
Amorphous SiO_2[37]		1.610 ± 0.01	32.4 ± 0.6	2.47	63

Nafion-MPTMS and Nafion-MPMDMS nanocomposite membranes to be interpreted as a measure of the fractal dimension of the inorganic network. Over the range $0.01 < q < 0.015$ Å^{-1} the curves have a slope of approximately -3.5, which indicates that the scattering objects in the size range $40 < R < 60$ nm have a mass fractal structure.

Nafion, Nafion-TEOS, and Nafion-MPMDMS composite membranes were studied by SANS and, under the same assumptions as for SAXS, the neutron SLD differences for Nafion-TEOS and Nafion-MPMDMS systems were calculated to be 1.7 and 2.6×10^{-6} Å^{-2}, respectively. Figures 5 and 6 show the neutron scattering profiles for Nafion-TEOS and Nafion-MPMDMS composite membranes, respectively.

Table 3 summarizes the peak positions, q_{max}, for the various curves and the corresponding real space distances, d. The peak position identified for Nafion in this work, $q = 0.19$ Å^{-1}, is slightly larger than that found in other investigations in which the membrane is swollen in water, such as $q = 0.13$ Å^{-1} [39] or $q = 0.12$ Å^{-1},[40] although this is to be expected as it is well-known that the ionic clusters of Nafion swell on exposure to polar solvents, leading to smaller q values for the ionomer peak.

Interestingly, the composite membranes show a shift in the ionomer peak position to even larger q values, at slightly less intensity than the Nafion peak. The higher q values indicate a reduction in the nearest-neighbor distance between ionic clusters, as shown in the lower d values in Table 3 for the Nafion composite samples. These values should be treated with some caution though, because as shown in Figures 5 and 6, the ionomer peak is quite broad and subject to some noise in the case of the composite samples, which makes determining the peak position difficult. Nevertheless, a clear distinction can be made between the peak position in Nafion and that in the Nafion composite samples, for which the separation between clusters is smaller for the composites.

The SANS scattering curves for Nafion-TEOS composite membranes show a significant increase at $q < 0.1$ Å^{-1}. The intensity of the increase is consistent with higher loadings of the inorganic component. This is a departure from the behavior seen with the SAXS scattering, in which there was little difference in the scattered intensity between the Nafion and the Nafion-TEOS composites (see Figure 2). However, it should be noted that X-rays are sensitive to differences in electron density (i.e., proportional to atomic weight), whereas in the case of Nafion composite membranes, neutrons are particularly sensitive to the hydrogen contribution to the scattering. The scattering of neutrons from the Nafion-MPMDMS samples also increases at lower q values, although the upturn occurs at lower q than for the Nafion-TEOS composites.

Wide-angle X-ray scattering in the range $q = 0.7-1.6$ Å^{-1} was used to obtain a measure of the crystallinity of Nafion, Nafion-TEOS, and Nafion-MPMDMS composite membranes. The measured curve was deconvoluted into two Gaussian peaks and a linear polynomial. The mean, variance, and magnitude of the Gaussian curves and the polynomial constants were used as fitting variables, and a least-squares fit between the measured data and the sum of the three curves was undertaken. The weight average crystallinity was then calculated according to eq 5,[38,41] in which I_{am} and I_{cr} are the intensities of the amorphous and crystalline peaks, respectively.

$$W_{cr} = \int_0^\infty I_{cr}(q)q^2\mathrm{d}q / \int_0^\infty [I_{cr}(q) + I_{am}(q)]q^2\mathrm{d}q \qquad (5)$$

The deconvoluted peak positions and calculated weight average crystallinities are summarized in Table 4. The positions of the crystalline and amorphous peaks for Nafion, determined in this work to be $q = 1.09$ Å^{-1} and $q = 1.22$ Å^{-1}, respectively, correspond well with the literature values of $q = 1.10$ Å^{-1} and $q = 1.24$ Å^{-1}.[41]

The results of the PALS experiments are listed in Table 5, including the literature values for Nafion and amorphous SiO_2. As can be seen for the Nafion 117 results, the result obtained in this work is consistent with the literature, and any difference is most likely due to differences in membrane pretreatment rather than experimental variations.

PALS has been used to study the free volume of PTFE/silica composite materials,[37] albeit with higher loadings than those used in this work. In that study, it was clearly shown that an increase in silica loading led to a linear increase in $\tau_3 I_3$ corresponding to the weighted average free volume. Interestingly though, in the present work. it was found that a simple linear relationship could not describe the relationship between the relative free volume fraction ($\tau_3 I_3$) and inorganic content, even with the inclusion of additional Nafion-MTES and Nafion-DMDMS membranes. Rather, as shown in Figure 7, the measured data varies widely from that predicted by a simple weighted average of $\tau_3 I_3$ for Nafion and amorphous silica.

(39) Gebel, G.; Lambard, J. *Macromolecules* **1997**, *30*, 7914.
(40) Rollet, A. L.; Gebel, G.; Simonin, J. P.; Turq, P. *J. Polym. Sci. Polym. Phys.* **2001**, *39*, 548.
(41) Fujimura, M.; Hashimoto, T.; Kawai, H. *Macromolecules* **1981**, *14*, 1309.

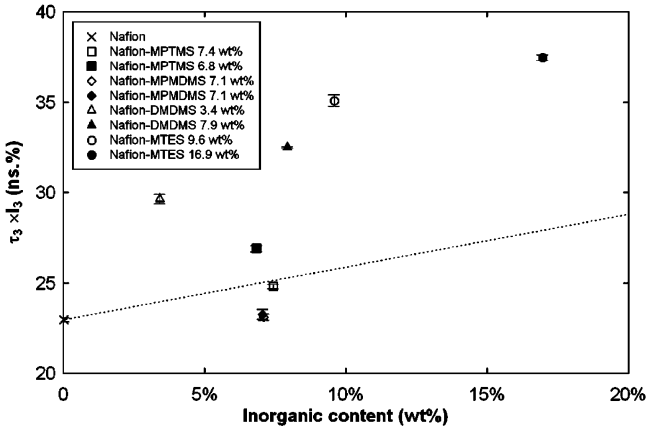

Figure 7. Relative free volume ($\tau_3 I_3$) as a function of inorganic loading for a range of Nafion nanocomposite membranes. The dashed line indicates the theoretical weight-averaged relative free volume for Nafion-SiO_2.

It is valid to construct such a graph using the weight percent on the abscissa, even though the relative free volume is a volumetric phenomenon, as the density of Nafion is approximately equal to that of amorphous silica.

For the purposes of rationalizing the PALS spectra of Nafion, consider it to be composed of three regions: the crystalline component, the amorphous component, and the hydrophilic cluster regions where the terminal sulfonic acid headgroups of the side chains aggregate. Chemically, the composition of the crystalline and amorphous regions of Nafion are the same as those in PTFE, as the side chains are excluded from this region. The PALS spectra of PTFE is commonly fitted with four finite lifetime components, attributed to annihilation of the following: p-Ps, $\tau_1 = 0.125$ ps; free (e+, not Ps) positrons, $\tau_2 = 300-500$ ps; o-Ps in crystals, $\tau_3 \approx 1$ ns; and o-Ps in amorphous regions, $\tau_4 = 2-6$ ns.[42,43] Nafion, on the other hand, is more often fitted with three lifetime components, with o-Ps annihilation in all regions (crystalline, amorphous, and ionic aggregate) responsible for $\tau_3 = 2.7-3.3$ ns.[44−47] Shantarovich et al.[48] attempted a four-component fit to Nafion; however, compared to a three-component fit, the relative errors in the lifetimes and especially the intensities were larger.

At 27 °C, Dlubek et al.[49] found the crystalline and amorphous free-volume domains of PTFE to have radii of 0.194 and 0.446 nm, respectively (using a four-component lifetime fit). When this is compared to the free-volume void size distribution calculated for Nafion by Sodaye et al.[46] using the CONTIN code,[50] it can be seen that the crystalline PTFE peak lies outside the left of the probability density function, and the amorphous PTFE peak to the right of the center of the peak. On the other hand, Ito et al.[51] measured the free volume of PTFE samples with varying crystallinity (30−90%) and found that for the highly crystalline sample, in which vacancies are expected to mostly arise from interstitial or interfacial voids in the crystals, the vacancies were in the range 0.30−0.32 nm (at 27 °C). This is in good agreement with the prediction of Sodaye et al.[46]

The contribution of the ionic aggregate region of Nafion to the PALS spectrum is unclear. Sodaye et al.[45] examined the free volume change in Nafion 117 that accompanied a change in size of the ionic cluster region and showed that increasing the cluster size led to smaller free-volume holes.

The interfacial region between the ionic cluster and the hydrophobic polymer backbone is not smooth. Despite the precise structure of these clusters remaining unknown, a recently proposed structure[52] suggests that numerous nanovoids may form at the interface between adjacent polymer chains forming the bounds of the region. As these clusters swell, the surface becomes bound by a larger number of polymer chains and the curvature is less severe, which should lead to a smoother (and less-free-volume containing) interface. This is consistent with the widely discussed Gierke model of the morphology of Nafion,[53] which predicts that as the clusters in Nafion grow, the number of exchanges sites per cluster increases. Geometrically, this is only possible if the cluster is bound by a larger number of chains so as to allow the side chains to coordinate into the cluster.

The crystallinity of Nafion is extremely sensitive to modifications in the polymer morphology. As shown in Table 4, the incorporation of even a small amount of inorganic filler leads to a large decrease in the polymer crystallinity, for example from 48% for Nafion to 25% for a Nafion-TEOS 1.3 wt % composite. This would consequently increase the number of free volume voids arising from the amorphous component. Provided the mean size of the free-volume holes arising from the amorphous region was smaller than that from the ionic aggregate, this would lead to a decrease in the overall mean free-volume size.

Scheme 1 presents a model of Nafion and three Nafion nanocomposite membranes.

The three systems chosen for this model were Nafion-TEOS, Nafion-MPTMS, and Nafion-MPMDMS, because of the systematic variations in the functionality of the silicon alkoxide precursor. TEOS is able to form up to four siloxane bonds with neighboring silicon atoms, whereas MPTMS can form three at most. Hence, both TEOS and MPTMS can form three-dimensional inorganic microstructures; however, in the case of MPTMS, the relatively long organic side chain produces significant steric hindrance to effective condensa-

(42) Dlubek, G.; Saarinen, K.; Fretwell, H. M. *Nucl. Instrum. Methods Phys. Res., Sect. B* **1998**, *142*, 139.
(43) Dlubek, G.; Sen Gupta, A.; Pionteck, J.; Hassler, R.; Krause-Rehberg, R.; Kaspar, H.; Lochhaas, K. H. *Polymer* **2005**, *46*, 6075.
(44) Shantarovich, V. P.; Novikov, Y. A.; Suptel, Z. K.; Kevdina, I. B.; Masuda, T.; Khotimskii, V. S.; Yampolskii, Y. P. *Radiat. Phys. Chem.* **2000**, *58*, 513.
(45) Sodaye, H. S.; Pujari, P. K.; Goswami, A.; Manohar, S. B. *J. Polym. Sci. Pol. Phys.* **1997**, *35*, 771.
(46) Sodaye, H. S.; Pujari, P. K.; Goswami, A.; Manohar, S. B. *J. Polym. Sci. Pol. Phys.* **1998**, *36*, 983.
(47) Sodaye, H. S.; Pujari, P. K.; Goswami, A.; Manohar, S. B. *Radiat. Phys. Chem.* **2000**, *58*, 567.
(48) Shantarovich, V. P.; Kevdina, I. B.; Yampolskii, Y. P.; Alentiev, A. Y. *Macromolecules* **2000**, *33*, 7453.
(49) Dlubek, G.; Saarinen, K.; Fretwell, H. M. *J. Polym. Sci. Polym. Phys.* **1998**, *36*, 1513.
(50) Gregory, R. B.; Zhu, Y. *Nucl. Instrum. Methods Phys. Res., Sect. A* **1990**, *290*, 172.
(51) Ito, Y.; Mohamed, H. F. M.; Seguchi, T.; Oshima, A. *Radiat. Phys. Chem.* **1996**, *48*, 775.
(52) Ioselevich, A. S.; Kornyshev, A. A.; Steinke, J. H. G. *J. Phys. Chem. B* **2004**, *108*, 11953.
(53) Gierke, T. D.; Munn, G. E.; Wilson, F. C. *J. Polym. Sci. Polym. Phys.* **1981**, *19*, 1687.

Scheme 1. Model of Nafion, Nafion-TEOS, Nafion-MPTMS, and Nafion-MPMDMS Nanocomposite Systems

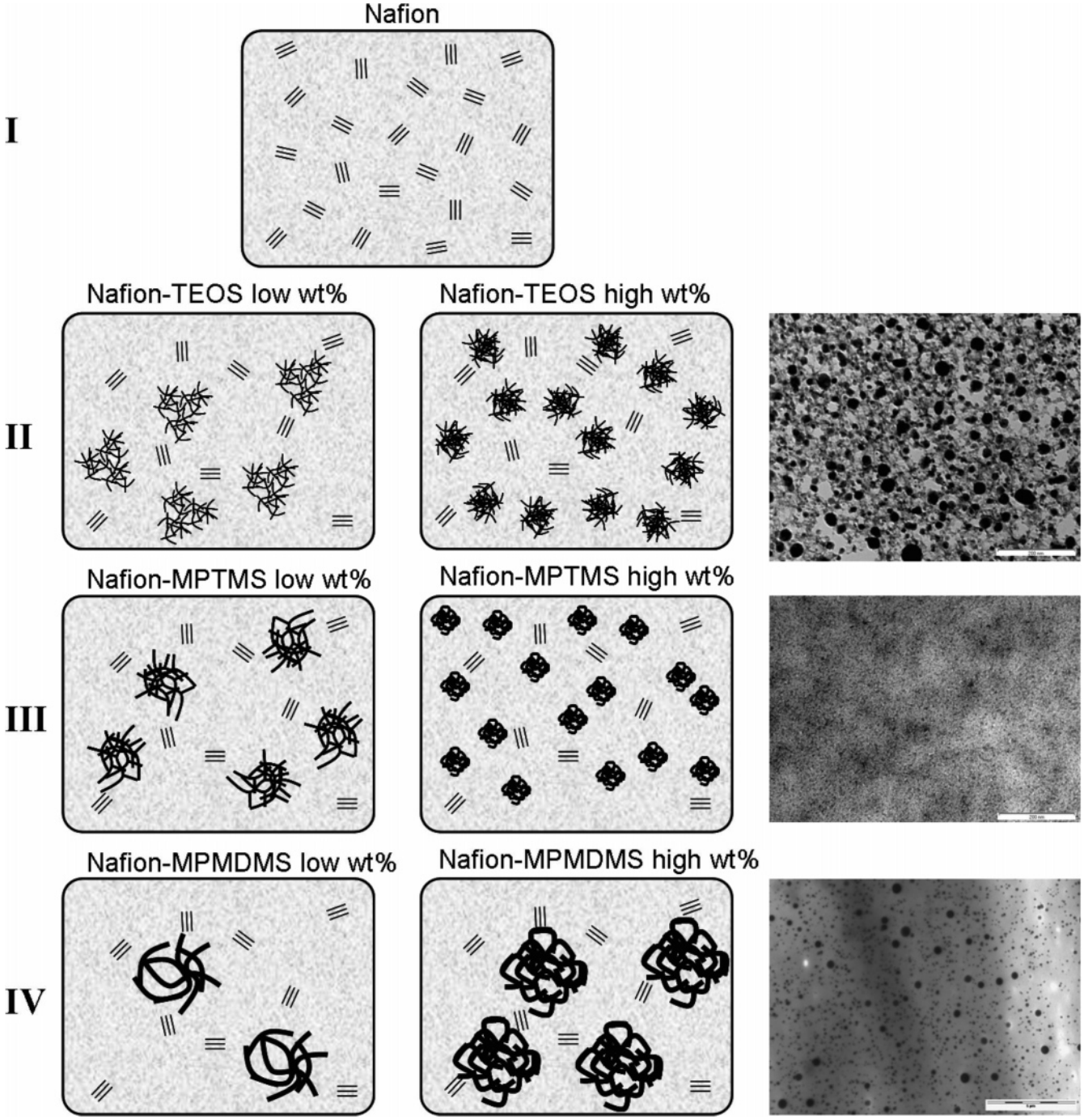

tion. This is seen particularly in the SAXS results for the Nafion-MPTMS composite membranes, in which a slope of approximately −3 in the $I(q)$ vs q plot indicates that the inorganic phase has a mass fractal structure.

The third inorganic precursor chosen for illustration in this model is MPMDMS. This precursor has two organic moieties (the propyl thiol group and a methyl group) covalently bound to the silicon atom, and so can form only two siloxane bonds. The only two-dimensional structure this precursor may form is a linear chain or possibly a closed ring; no covalently bonded three-dimensional structure is possible. However, it was shown, particularly by TEM micrographs, that MPMDMS forms quite large (50−200 nm) particlelike agglomerates of inorganic chains.

The first image (I) presented in Scheme 1 is that of unmodified Nafion. The background pattern, which appears mottled, represents the fine structure of the Nafion polymer at a scale of approximately 30−35 Å separation between ionic clusters. This separation distance is well-known from the literature and was confirmed experimentally in this work by SANS. The other key feature presented in the depiction of Nafion is the significant crystallinity (the crystallites are represented by clusters of three straight lines), which was shown by WAXS to be significantly reduced in all of the nanocomposites.

The second series of images (II) in Scheme I represent Nafion-TEOS composites at low and high loadings. The constituent units of the agglomerates shown are monomers

Table 6. Proton Conductivity, Methanol Permeability, and Selectivity Data for Nafion and Selected Nafion Nanocomposite Membranes at 50 °C

sample	inorganic content (wt %)	σ (mS cm^{-1})	P_M ($\times 10^{-6}$ cm^2 s^{-1})	β ($\times 10^6$ mS cm^{-3})
Nafion 117		17.7	2.91	6.08
Nafion-TEOS	8.5	13.2	3.33	3.96
Nafion-TEOS	15.3	13.7	3.07	4.47
Nafion-TEOS	17.5	10.7	2.67	4.02
Nafion-MPTMS	4.5	14.0	3.10	4.50
Nafion-MPTMS	9.2	13.8	3.08	4.50
Nafion-MPTMS	16.5	10.0	2.43	4.13
Nafion-MPMDMS	10.8	6.9	0.358	19.1
Nafion-MPMDMS	14.9	6.7	0.311	21.5
Nafion-MPMDMS	16.7	5.6	0.308	18.1

representative of fully hydrolyzed TEOS. At low loading, they agglomerate to form aggregates, although the degree of condensation is not high (as shown by ICP-AES analysis). Quite an important feature of the composite membrane, as compared to Nafion, is the significantly reduced crystallinity, as indicated by the reduced number of crystallites. This was considered the primary reason for the larger free volume of Nafion-TEOS composites compared to Nafion. The Nafion-TEOS membrane with a higher loading shows the agglomerates as more dense particles, consistent with the higher degree of condensation of the silicon oxide network, and of course the overall number quantity of inorganic material is higher. This can be compared to the TEM image at the right, which is a Nafion-TEOS composite membrane of around 10 wt % loading (the scale bar is 200 nm). The particles appear quite dense and reasonably circular in shape and, importantly, quite large (the majority have a diameter larger than 20 nm). This explains the SAXS results for the Nafion-TEOS composite membranes. in which little contribution to the scattering was seen from the silicon oxide phase, because the particles are too large to have an effect in the q range studied in this work.

The third series of images (III) represent Nafion-MPTMS composite membranes. Similar to the Nafion-TEOS images, the constituent units of the agglomerates are the fully hydrolyzed silicon alkoxide precursors. The difference is that these precursors have a propyl-thiol functional group attached to the silicon atom and can hence form only three siloxane bonds, which are represented as three small arms on each unit. These units agglomerate to form moderately condensed units at low loading, and at high loading they condense almost completely. As for the Nafion-TEOS composites, the crystallinity is significantly reduced in the Nafion-MPTMS composites, which was reflected in the PALS results. The TEM image, which again shows an approximately 10 wt % composite, indicates a fine homogeneous dispersion of the inorganic phase throughout the polymer structure. This is likely due to the sulfonic acid groups on the agglomerate outer surface compatibilising the inorganic particles with the ionic cluster regions of the Nafion matrix.

The final series of images (IV) in Scheme I represent Nafion-MPMDMS nanocomposite membranes. This precursor forms only linear chains when condensed, and so the agglomerates shown are formed accordingly. As for the other two composite systems, the crystallinity of the polymer phase is significantly reduced compared to Nafion. In both low and high loading systems, the precursor is quite significantly condensed, as was shown by ICP-AES; however, the main difference lies in the extent of aggregation between the two. At high loading, the linear chains cluster together quite significantly to form large clusters, although there is quite a high degree of polydispersity in the system. That is, when examining the micrograph shown at the right, it can be seen that there is a wide range of particle sizes. This leads to a large upturn in the SAXS intensity toward lower q values as seen in Figure 4.

The proton conductivity and methanol permeability of Nafion 117 and a selection of Nafion nanocomposite membranes are listed in Table 6. The selectivity, β, is defined as the ratio of proton conductivity to methanol permeability and used as a guide to the suitability of a given membrane for use in the direct methanol fuel cell.[54] The concentration of the permeating methanol/water solution used in this work was much higher than that used in typical DMFCs, which employ much lower concentrations, around 0.5−2.0 M to mitigate methanol crossover. It is possible that the membranes may have suffered from excessive swelling during testing, and future work will examine the use of lower concentration permeation feed solutions. Methanol/water uptake and dimensional swelling experiments may also be conducted in future to better correlate transport and structural results.

All of the composite membranes displayed a lower proton conductivity than Nafion, indicating that the presence of the inorganic particles and agglomerates has disrupted the proton-transfer pathways. Furthermore, as the inorganic loading is increased, the proton conductivity decreases further. The Nafion-TEOS and Nafion-MPTMS composite membranes with lower inorganic contents had higher methanol permeabilities than Nafion; however, at higher loadings (17.5 and 16.5 wt %, respectively) their methanol permeability was lower than that of Nafion. Nafion-MPMDMS nanocomposite membranes, however, had particularly low methanol permeabilities, almost an order of magnitude lower than that of Nafion; despite their proton conductivity being lower than that of Nafion, they still produced selectivity values more than three times higher than Nafion. As was shown in Figure 7, Nafion-MPMDMS nanocomposite membranes exhibited the lowest relative free volume of the composite systems tested. Furthermore, as presented in the discussion of the model in Scheme 1, the inorganic network in the Nafion-MPMDMS system has a highly branched fractal structure, highly compatibile with the polar cluster regions of Nafion because of the sulfonic acid functionalized inorganic structure. It is proposed that the methanol permeability of the Nafion-MPMDMS composite membranes is so significantly reduced because of the interpenetrated nature of the composite system, dramatically increasing the tortuosity for methanol molecules diffusion, whereas the proton conductivity is only slightly reduced because of the additional proton-transfer sites provided by the sulfonic acid sites in the inorganic network.

(54) Li, X.; Roberts, E. P. L.; Holmes, S. M. *J. Power Sources* **2006**, *154*, 115.

Conclusions

Analysis of the silicon content of composite membranes by ICP-AES suggests that at low inorganic loadings, there is only a moderate degree of condensation of the silicon alkoxide precursor. At higher loadings, however (around 10 wt % and above), the degree of condensation is quite significant.

Wide-angle X-ray scattering revealed that there is a significant reduction in the polymer crystallinity from around 48% in Nafion to 25−30% in the composite membranes.

Small-angle X-ray scattering revealed major differences in the scattering behavior of Nafion-TEOS, Nafion-MPTMS, and Nafion-MPMDMS composite membranes. There was little difference between the scattering curves of Nafion and the Nafion-TEOS composite membranes, most likely due to the fact that the particle size observed for these materials using TEM was larger beyond the q range studied. The Nafion-MPTMS and Nafion-MPMDMS composites showed a strong upturn in the scattered intensity at low q however, with the slope of the linear region being around −3. This corresponds to an inorganic mass fractal structure, which was confirmed by TEM images showing a nonsmooth particle surface that was significantly interpenetrated by the polymer phase. This structure was also consistent with the predicted inorganic structures that may form from these precursors.

Small-angle neutron scattering was able to resolve the ionomer peak of the Nafion and Nafion composite membranes. There was a broadening of the peak and a reduction in intensity for all the composites, suggesting that the inorganic phase has disrupted the orderly formation of the ionic clusters. The calculated diameter of the clusters was also slightly reduced in the composites.

Positron annihilation lifetime spectroscopy proved an excellent tool for the study of Nafion composite membranes. It was shown that incorporating silicon oxide led to an increase in the o-Ps lifetime and intensity. The order of the increase by silicon alkoxide precursor was MPMDMS < MPTMS < DMDMS < MTES. The increase in the polymer free volume with incorporation of the inorganic particles was rationalized in terms of the change in crystallinity of the materials, as the free volume of the amorphous region is significantly higher than that of the crystalline region.

Finally, a structural model for Nafion-TEOS, Nafion-MPTMS, and Nafion-MPMDMS composite membranes was proposed that well-described the characterization carried out on these samples and their relationship with the transport properties measured.

Acknowledgment. The authors gratefully acknowledge the financial support of the Australian Research Council under the ARC Centres of Excellence Program and the Federation Fellowship for G.Q.L. Use of the ChemMatCARS Sector 15 at the Advanced Photon Source was supported by the Australian Synchrotron Research Program, which is funded by the Commonwealth of Australia under the Major National Research Facilities Program. ChemMatCARS Sector 15 is principally supported by the National Science Foundation/U.S. Department of Energy under Grant CHE0087817 and by the Illinois Board of Higher Education. The Advanced Photon Source is supported by the U.S. Department of Energy, Basic Energy Sciences, Office of Science, under Contract W-31-109-Eng-38.

CM0628698